SCIENTIFIC REPORTS

OPEN

SUBJECT AREAS:
SPINTRONICS
MAGNETIC PROPERTIES AND MATERIALS
FERROMAGNETISM
ELECTRONIC PROPERTIES AND MATERIALS

Received
8 November 2012

Accepted
25 April 2013

Published
14 May 2013

Correspondence and requests for materials should be addressed to P.J.M. (peter.metaxas@uwa.edu.au)

High domain wall velocities via spin transfer torque using vertical current injection

Peter J. Metaxas[1,2], Joao Sampaio[1], André Chanthbouala[1], Rie Matsumoto[1,3], Abdelmadjid Anane[1], Albert Fert[1], Konstantin A. Zvezdin[4,5,6], Kay Yakushiji[3], Hitoshi Kubota[3], Akio Fukushima[3], Shinji Yuasa[3], Kazumasa Nishimura[7], Yoshinori Nagamine[7], Hiroki Maehara[7], Koji Tsunekawa[7], Vincent Cros[1] & Julie Grollier[1]

[1]Unité Mixte de Physique CNRS/Thales and Université Paris-Sud 11, 1 Ave. A. Fresnel, 91767 Palaiseau, France, [2]School of Physics, M013, University of Western Australia, 35 Stirling Highway, Crawley WA 6009, Australia, [3]National Institute of Advanced Industrial Science and Technology (AIST) 1-1-1 Umezono, Tsukuba, Ibaraki 305-8568, Japan, [4]A. M. Prokhorov General Physics Institute of RAS, Vavilova str. 38, 119991 Moscow, Russia, [5]Moscow Institute of Physics and Technology, 141700, Institutskii, 9, Dolgoprudny, Moscow Region, Russia, [6]Istituto P. M. s.r.l., via Cernaia 24, 10122 Torino, Italy, [7]Process Development Center, Canon ANELVA Corporation, Kurigi 2-5-1, Asao, Kawasaki, Kanagawa 215-8550, Japan.

Domain walls, nanoscale transition regions separating oppositely oriented ferromagnetic domains, have significant promise for use in spintronic devices for data storage and memristive applications. The state of these devices is related to the wall position and thus rapid operation will require a controllable onset of domain wall motion and high speed wall displacement. These processes are traditionally driven by spin transfer torque due to lateral injection of spin polarized current through a ferromagnetic nanostrip. However, this geometry is often hampered by low maximum wall velocities and/or a need for prohibitively high current densities. Here, using time-resolved magnetotransport measurements, we show that vertical injection of spin currents through a magnetic tunnel junction can drive domain walls over hundreds of nanometers at ~500 m/s using current densities on the order of 6 MA/cm². Moreover, these measurements provide information about the stochastic and deterministic aspects of current driven domain wall mediated switching.

Via the injection of spin polarized current, spin-transfer-torques (STT) allow for the manipulation or switching of a ferromagnetic nanostructure's magnetization configuration without the use of an externally applied magnetic field[1,2]. One way for this switching to occur is through controlled domain wall motion, which can be driven by injecting current laterally along a nano-scale ferromagnetic strip containing one or more domain walls[3–6]. This ability to displace domain walls via current has driven strong research efforts into scalable, spintronic, domain wall-based devices such as shift registers[7–11], binary memories[12–14] and memristors[15–17].

In the conventional lateral current geometry, the non-adiabatic spin torque that drives steady state domain wall motion[18,19] is intrinsically small[20–22], generally limiting the domain wall speed to below 150 m/s[22–24] and requiring current densities above 100 MA/cm², a value which can be prohibitive for applications[7]. Recent results have shown that the domain wall velocity can be strongly enhanced by the addition of a metallic layer with strong spin-orbit coupling below the ferromagnetic strip[25–27]. Nevertheless, in these latter systems the current densities required to move the wall at high speed are still high (~100 MA/cm²) and the physical interpretation of the observed effects remain complicated since spin orbit coupling can also affect the domain wall structure and thus its dynamics[28].

Recently we proposed an alternative way to enhance the driving torque for domain wall motion through the use of vertical (or 'perpendicular') current injection through a magnetic tunnel junction consisting of a fixed magnetic layer which acts as a spin polarizer and a 'free' magnetic layer containing a domain wall. In this injection geometry, the current densities required to move the domain walls are reduced by up to two orders of magnitude[16] and it has been predicted that wall velocities could exceed 400 m/s at current densities as low as a few MA/cm²[29].

In this article, we carry out precise measurements on both stochastic and high speed deterministic domain wall dynamics under perpendicular current injection[16,30–35] by performing real-time measurements of domain

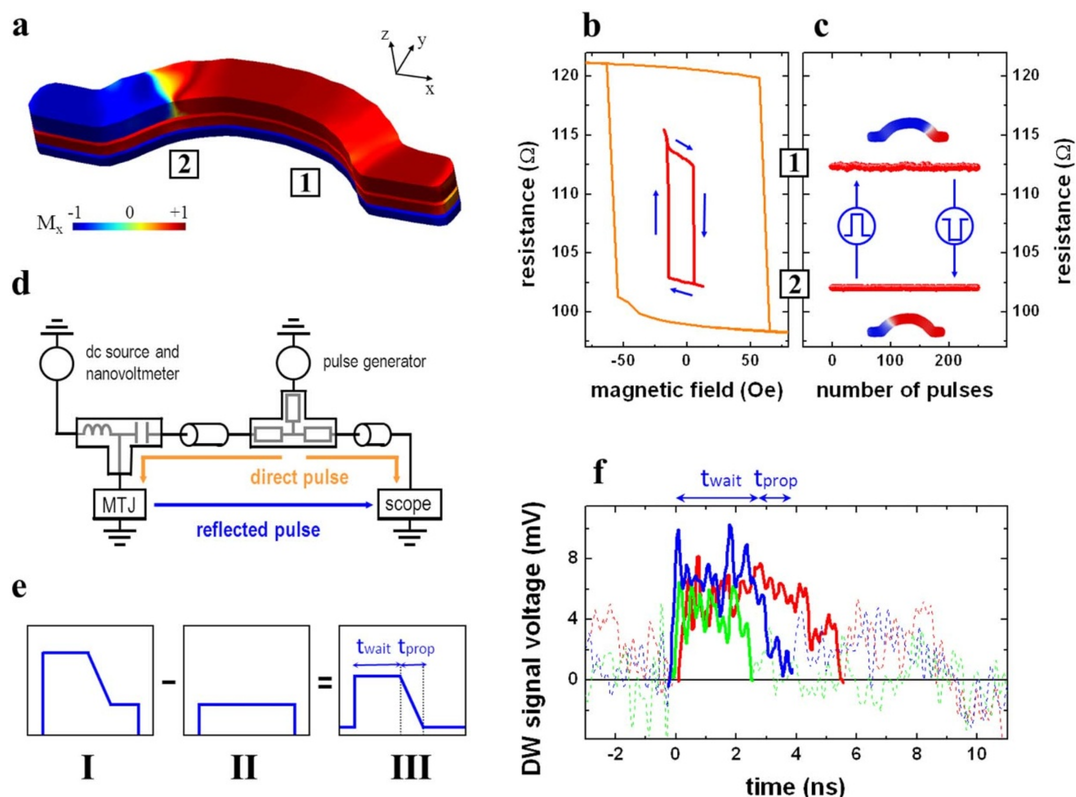

Figure 1 | Measurements of domain wall mediated resistance switching under field and vertically injected current. (a) Schematic of the MTJ stack with the domain wall in one of the two labeled, stable positions. (b) Typical resistance versus magnetic field curves during reversal of the free NiFe layer measured using a non-perturbing sense current of $I_{sense} = 100\ \mu A$. The orange curve shows switching between the fully parallel and antiparallel states. The red curve corresponds to the changes in the device resistance upon cycling the domain wall back and forth between the two stable domain wall positions, 1 and 2, near the terminations of the arc. (c) Current-induced back-and-forth displacements between positions 1 and 2 upon application of 20 ns long voltage pulses with $J \sim 7.3$ MA.cm^{-2}. Insets: top view of micromagnetically simulated stable DW configurations. (d) Schematic of the setup used for the time resolved reflective measurement method. (e) Domain wall voltage traces (panel III) are obtained by recording the reflected voltage pulse during which the domain wall moves from one termination to another (panel I) and subtracting from it the reflected voltage pulse obtained when the wall is trapped at the second termination (panel II). (f) Single-shot voltage traces obtained under 20 ns long sub-critical current pulses ($J \sim 0.7 J_C$). The parts of the traces occurring before the pulse and after the voltage signal has returned to zero are dashed to highlight the part of the trace corresponding to the waiting and propagation processes. The waiting and propagation times are labeled for the 'central' blue trace ($t_{switch} = t_{wait} + t_{prop} \sim 4$ ns).

wall-mediated magnetization switching within the free layer of arc shaped nano-scale MgO-based MTJ devices (Figs. 1a–e). These structures provide an ideal base architecture for data storage and memristive devices because the strong tunneling magnetoresistance[36,37] translates small domain wall displacements in the free layer into large resistance changes of the device as a whole[38]. These large resistance variations are also ideal for probing high speed magnetisation dynamics[39].

Results

The measured MTJ devices have the following general composition wherein a synthetic antiferromagnet (SAF) is used as a current polarizer: SAF/MgO(1.17 nm)/NiFe(5 nm) (see methods for full device structure). Each device is in the shape of an arc of ~115 nm width with horizontal terminations at each end (Fig. 1a). To create a transverse[40] domain wall (DW) within the NiFe layer, we apply a large in-plane field perpendicular to the long axis of the device. A domain wall is created at the apex of the arc and then, in zero field, relaxes to a stable position near one of the horizontal terminations which serve to constrain the domain wall inside the arc. Each one of these positions (referred to as positions 1 and 2) is well reproduced by micromagnetic simulations (see Figs. 1a and 1c) and corresponds to a discrete resistance level due to the device's TMR (Figs. 1b and 1c).

A prepared domain wall can be driven back and forth between positions 1 and 2, thus switching the device between the two discrete resistance states. This can be done either via the application of a field along the long axis of the device or vertical current injection in zero external field. Fig. 1b demonstrates the field induced switching wherein the field is cycled between positive and negative values whilst monitoring the sample resistance. Notably, after displacing the wall to either of the two positions, it is stable at remanence in zero field. The application of negative (positive) current pulses can also be used to drive the transition $1 \rightarrow 2$ ($2 \rightarrow 1$) in zero applied field. Fig. 1c shows a series of measurements of the device's resistance made directly following the application of alternating positive and negative vertically injected current pulses with $J \sim \pm 7.3$ MA.cm^2 and duration 20 ns. We thus demonstrate that the domain wall mediated switching can be carried out repeatedly using injected current pulses without the use of an external magnetic field.

In the remainder of this article, we concentrate on magneto-transport experiments carried out to probe the dynamics of the domain wall during its motion between the two terminations. Notably, we show that the switching can be deterministic and that the propagation occurs at velocities on the order of 500 m/s corresponding to device switching on the order of 1 ns with negligible switching stochasticity.

A schematic of the measurement circuit is given in Fig. 1d. We use a reflection technique where we send a pulsed current through the MTJ and measure the reflected voltage pulse. For a domain wall prepared at position 1, a negative current pulse will displace it to

position 2 (Fig. 1c). Its displacement will result in an instantaneous drop in the sample resistance and thus also in the magnitude of the reflected voltage pulse (panel I of Fig. 1e). A second, identical voltage pulse is then sent through the sample however the wall does not appreciably move due to the termination-induced confinement. The reflected voltage pulse is again recorded (panel II of Fig. 1e) and used as a reference trace which is subtracted from the first trace to yield a domain wall voltage signal such as that shown in panel III of Fig. 1e. We note that the device resistance is measured before and after both the driving and reference pulses using a non-perturbing 100 μA sense current in order to verify the domain wall's position at each step of the experiment.

Three measured domain wall voltage traces obtained under a single sub-critical current density ($J \sim 0.7 J_C$) are shown in Fig. 1f. The subtracted voltage signal is zero before the pulse, and then plateaus during a stochastic waiting or depinning time, t_{wait}, wherein the wall does not measurably move. Finally, a drop in the signal is observed, corresponding to the domain wall traveling to the other end of the device during a time t_{prop}. The full switching time of the device is thus given by $t_{switch} = t_{wait} + t_{prop}$. At higher current densities, as will be shown below, the switching time is on the contrary determined almost exclusively by the propagation time corresponding to an abrupt change in the voltage trace.

The voltage drop corresponding to the domain wall propagation occurs rapidly with t_{prop} on the order of 1 ns. To obtain a clearer visualization of these fast propagation dynamics, we recorded $\sim$100 real time voltage traces, and plotted them as V versus $t - t_{switch}$ where t_{switch} was measured manually. The curves were then averaged to reduce the signal noise during the propagation part of the curve. These averaged shifted traces for three values of J are shown in Fig. 2a from which an upper bound for t_{prop} can be estimated to be $\sim$1.5 ns. This corresponds to an average domain wall velocity on the order of 400 m.s^{-1} given that the propagation distance is $\sim$600 nm. This result can be compared to those obtained from micromagnetic simulations (see methods) shown in Fig. 2b which show the spatially averaged longitudinal component of the free layer magnetization during current driven domain wall motion. The plotted magnetisation component is representative of the resistive change induced during domain wall motion. By also shifting these simulated curves by t_{switch} it can be seen that the simulated and measured propagation times are in good agreement. Moreover, the simulation indicates that the maximum velocity during propagation can reach 600 m/s.

Despite these fast dynamics, at sub-critical current densities the waiting times preceding the domain wall propagation are characterized by significant variability, as seen directly in Fig. 1f. However, these waiting times become immeasurably small above the critical current density. To demonstrate the transition from sub-critical thermally activated domain wall dynamics towards deterministic dynamics, we measure the characteristic domain wall mediated switching time as a function of J as extracted from averaged voltage traces ($\sim$200 single shot traces per averaged trace). The averaged traces were obtained under 20 ns long pulses for different current densities with $J > 0$ and are shown in Fig. 2c. Here, there was no horizontal shift of the traces along the time axis (as done in Figs. 2a and 2b) and so these averaged traces probe the entire switching process: both stochastic depinning and propagation. At low current densities it is clear that the characteristic waiting time is much longer than the propagation time (typically 1–1.5 ns as shown earlier).

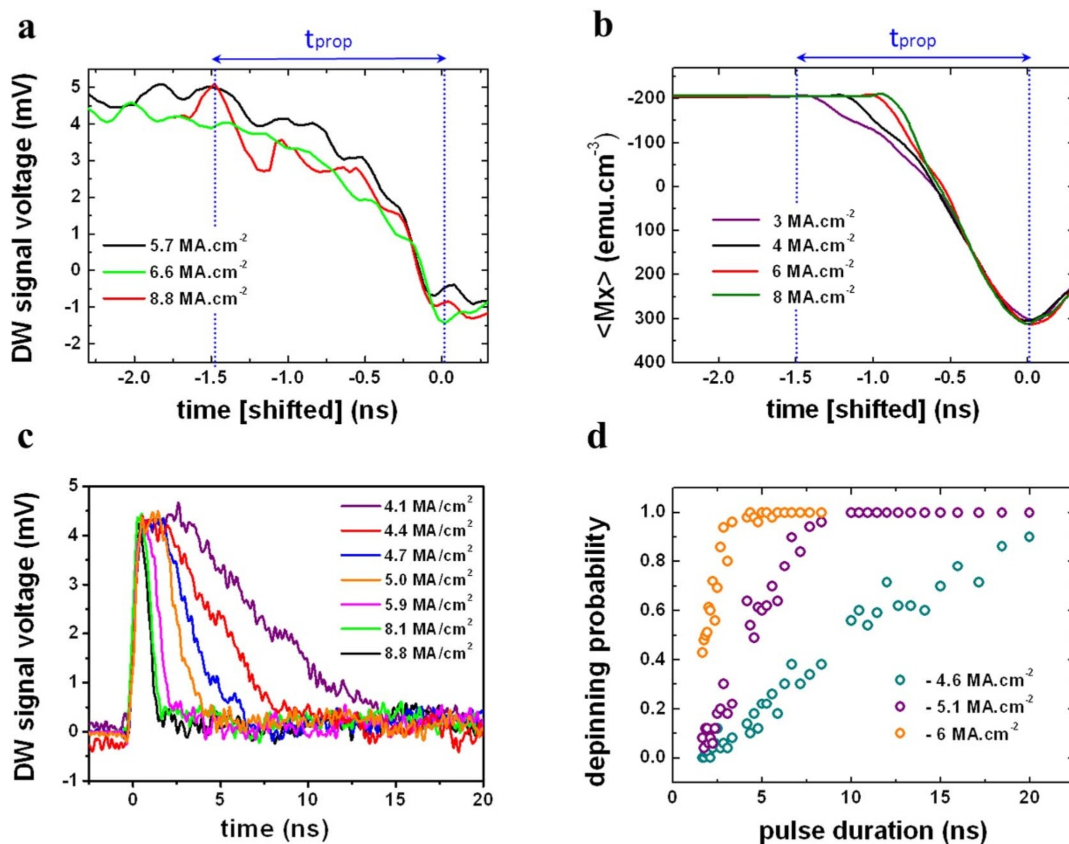

Figure 2 | Domain wall propagation, switching and depinning times. (a) The propagation time t_{prop} is measured by averaging several single-shot traces shifted by $t - t_{switch}$. The resulting traces are shown for different current densities and reveal $t_{prop} \sim 1$ ns. (b) Micromagnetic simulations: the average x component of the magnetization is equivalent to the resistive change due to the domain wall displacement. (c) Averaged single shot DW voltage traces for several current densities at a constant pulse duration of 20 ns. (d) Depinning probability as a function of pulse duration for different current densities in a second device.

Indeed the low J traces can be decomposed into two parts. First because of the low probability of switching events, the voltage remains constant. The voltage then decreases towards $V = 0$ with a smeared, sloping transition indicative of a wide distribution of t_{wait} times which dominate the switching characteristics and limit switching reliability. As the current density is increased however, the switching transition is faster and the waiting time reduced, resulting in strongly diminished plateau widths at the beginning of the averaged traces. At current densities above approximately 6 MA.cm^{-2} (green and black curves in Fig. 2c) there is no measurable waiting time and the motion is consistent with a deterministic motion with $t_{switch} \sim t_{prop}$. Additional averaged traces are given in Supplementary Fig. S1.

Conventional depinning probability measurements were carried out on a second device with the same structure where the probability of observing a depinned domain wall was measured following the application of a pulse with a given current density and variable duration. Data is shown in Fig. 2d where we plot the depinning probability versus pulse duration. Although these measurements only probe t_{wait}, we observe consistency with the the averaged voltage traces presented in Fig. 2c in that for a given pulse duration, the depinning probability increases with J. Alternatively, it is possible to normalize and invert the domain wall voltage traces from Fig. 2c to generate curves which show the probability of the domain wall having both depinned and traveled to the other side of the device under the action of a continuously applied current pulse. When $t_{prop} << \bar{t}_{wait}$ (ie. at low J), the averaged voltage traces and conventional depinning probability measurements compare well (Fig. 3a). At higher J, the depinning probability increases faster than the switching probability (Supplementary Fig. S2), consistent with the fact that the switching measurements probe both the depinning and propagation times.

Since it is the full switching time, $t_{prop} + t_{wait}$, which is of importance for device operation, we use the inverted, averaged domain wall voltage traces to extract a mean switching time τ as a function of J. To do this, we fit the inverted and rescaled data with a statistical cumulative distribution function which describes the probability of the device having switched at a given time t. The existence of a plateau at the start of the low J averaged traces does not permit the use of the exponential probability distribution function, often employed for magnetic switching in cases where $t_{prop} \ll t_{wait}$[41,42]. Instead, we use the gamma statistical distribution, a flexible 2 parameter model which can be employed to model waiting times[43]. Notably this distribution can be used to fit the broad voltage traces observed at low J where stochasticity dominates as well as the sharply varying traces obtained at high J in Fig. 2c. The extracted values of τ (see methods) are given in Fig. 3b where we plot ln τ versus J. A simple linear fit to the low J data highlights the existence of two regimes, one below and one above a critical current density of ~6 MA/cm^2. This value appears to be quite consistent with the averaged voltage traces where we see that at approximately 6 MA/cm^2 the plateau in the averaged traces disappears. Furthermore, at this point, the drop in the voltage occurs over a time frame consistent with the measured and simulated t_{prop} values (Figs. 2a and 2b). Indeed, at the highest measured current density, the domain wall signal voltage drops to zero in a time close to 1 ns, indicative of domain wall velocities approaching 600 m/s. A more rigorous analysis of the ln τ versus J data is discussed below where we extract a value for the effective field arising from the STT.

Discussion

Finite, pre-switching waiting times have been observed both below and above the critical current for STT induced uniform magnetic switching[42,44], the latter being due to a zero torque when the magnetizations of the free and polarizing layers are aligned. In our system however, the spins in the transverse domain wall always form an angle with the magnetization of the polarizing layer, resulting in a finite initial torque. The waiting times for domain wall propagation that are observed here thus simply indicate that the applied current density is sub-critical, meaning that thermal activation is required to overcome the domain wall pinning energy and initiate motion.

The J dependence of τ can be understood by considering a transition from thermally activated to deterministic domain wall dynamics[42]. The characteristic time associated with thermally activated depinning can be expressed as

$$\tau \propto \exp(E_B/k_B T) \tag{1}$$

with the following expression for the energy barrier[41,45]

$$E_B \propto \left(1 - H_J/H_{dep,T=0}\right)^{\frac{3}{2}}, \tag{2}$$

which is defined only for $H_J \leq H_{dep,T=0}$. $H_{dep,T=0}$ is the depinning field at zero temperature. $H_J = H_{STT} + H_{Oe}$ is the equivalent field corresponding to the net effect of the injected current, ie. the out-of-plane torque[29], H_{STT}, and the Oersted field[16], H_{Oe}, which both drive domain wall motion in our system. In the plot of τ versus J in Fig. 3b we can identify two regimes. In the under-critical regime $J < J_c$, the domain wall overcomes the energy barrier E_B with the help of thermal activation resulting in a distribution of waiting times as a consequence of the stochastic depinning process. The low J data in this regime is well fitted using Eqs. (1) and (2) from which a value of J_C = 5.9 MA.cm^{-2} can be directly extracted assuming an equivalence of J and H. When the current is strong enough, H_J equals $H_{dep,T=0}$ and

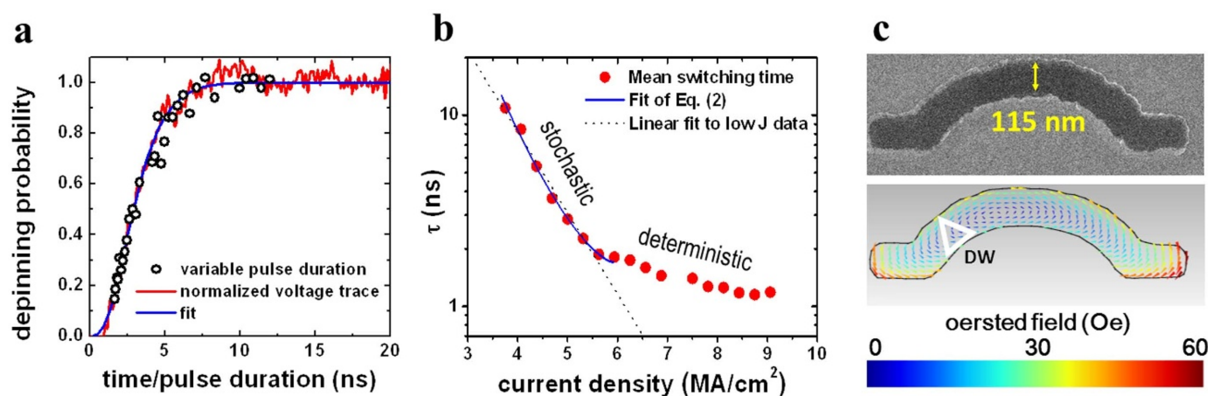

Figure 3 | Determination of the critical current for the transition from thermally activated to deterministic domain wall motion. (a) Comparison between the depinning data, switching probability data and a Gamma cumulative distribution function fit ($J = -5.45$ MA/cm^2). (b) Mean switching times extracted by fitting the Gamma cumulative distribution function to inverted and scaled time resolved DW signal voltage traces. (c) SEM image of the sample and simulated Oersted field taking into account the contribution from the current distribution within the electrodes.

the depinning process becomes deterministic with no appreciable or measurable waiting time. Even above J_C, τ continues to decrease with increasing J, which is indicative of a faster movement out of the stable domain wall position (as observed in the simulations shown in Fig. 2b) and thus a reduced $t_{switch} \sim t_{prop}$.

It is possible to extract the efficiency of the spin transfer out-of-plane torque from the thermally activated model using $H_J = H_{STT} + H_{Oe}$. We have calculated the amplitude and spatial distribution of H_{Oe} by taking into account the actual current distribution through the MTJ stack and the electrodes (see Supplementary Note S1). The net effect of H_{Oe} was found to aid domain wall depinning. Although the Oersted field can be rather strong in the terminations (up to 60 Oe for $J = 6$ MA.cm^{-2}, see Fig. 3c), its net effect is quite low at the pinned domain wall position. Simulations of domain wall depinning from position 1 under the influence of H_{Oe} only yielded an equivalent magnetic field per unit current density of 1.12 Oe.MA^{-1}.cm^2. Therefore the Oersted field results in an effective field acting on the domain wall of $H_{Oe} \approx 6.6$ Oe at J_C. A lower bound was also estimated for the zero temperature depinning field by extrapolating temperature dependent depinning measurements with $H_{dep}|_{T=0} \sim 27$ Oe (see Supplementary Note S2). As found previously in quasi-static measurements[16], this value confirms the two orders of magnitude gain compared to domain wall motion induced by non-adiabatic torque in the traditional lateral injection geometry, for which the equivalent field at the same current density is typically 0.1 Oe[46].

We have experimentally demonstrated domain wall propagation in a MTJ at velocities on the order of 500 m.s^{-2} under perpendicular current injection in the absence of an applied magnetic field. Real time magnetotransport measurements have allowed for an analysis of the transition between stochastic and deterministic domain wall dynamics which is crucial for any type of domain wall based device. At current densities above the critical current density ($\sim$6 MA.cm^{-2}), the device switching proceeds quickly with no measurable waiting time. This performance compares well with state-of-the-art uniform switching in MTJs[42] and with theory[29] suggesting that a factor of about five in efficiency could be gained by using a polarizer which is perpendicular to the magnetization of the free layer. In future applications, device sizes could be further reduced using materials with perpendicular magnetic anisotropy to decrease the domain wall width by an order of magnitude. This could allow for device dimensions on the order of 25 × 100 nm^2 leading to sub mA critical currents. The vertical current injection geometry in magnetic tunnel junctions is therefore extremely promising for future high speed domain wall based spintronic devices such as memristors and magnetic memories.

Methods

Samples. MTJ devices were fabricated from a multilayer film having the following composition PtMn(15 nm)/CoFe(2.5 nm)/Ru(0.9 nm)/CoFeB(3 nm)/MgO(1.17 nm)/NiFe(5 nm)/Ru(10 nm) which was sputtered in a Canon ANELVA chamber. Details of the growth and fabrication process have been presented elsewhere[47]. The samples were annealed at 0.5 T at 285°C during 6 hours and patterning carried out using electron beam lithography and ion beam etching. The tunneling magnetoresistance of the patterned devices is on the order of 25%, with a low RA product of $\sim$12 $\Omega.\mu m^2$. In our convention, a positive current favors the anti-parallel state.

Micromagnetic simulations. Dynamic simulations of the domain wall motion under the influence of perpendicularly injected current were carried out using the finite difference micromagnetic code, SpinPM, which was developed at Istituto PM srl. The simulated device had the geometry extracted from the SEM image in Fig. 3c and took into account the nonvertical device edges induced by the etching process. The following magnetic parameters were used: cell size of 3 × 3 × 5 nm^3, $\alpha = 0.01$ for the magnetic damping parameter, $M_S = 500$ emu/cm^3 for the free layer magnetization and respectively $M_S = 740$ emu/cm^3 and 690 emu/cm^3 for the top and bottom ferromagnetic layers in the synthetic antiferromagnet. The interlayer exchange coupling between the top layer of the synthetic antiferromagnet and the free layer was set to 0.0025 erg.cm^{-2}. The coupling between the layers within the synthetic antiferromagnet was set to -0.1 erg.cm^{-2}. The current was assumed to be uniform throughout the structure and a spin polarization of 0.5 was used.

Gamma distribution. The Gamma probability distribution function is given by

$$P(t) = \frac{t^{\alpha-1}\exp(-t/\beta)}{\Gamma(\alpha)\beta^{\alpha}} \tag{3}$$

where $\Gamma(\alpha) = \int_0^\infty y^{\alpha-1}\exp(-y)\,dy$ is the conventional Gamma function. α and β characterize the form of the distribution with the Gamma and exponential distribution functions being equivalent for $\alpha = 1$. The inverted and normalized averaged voltage traces were fitted with the cumulative distribution function of the gamma distribution using the CDF, GammaDistribution and FindFit functions built into Wolfram Mathematica. This allowed α and β to be determined for each value of J. We then calculated the mean of the distribution, $\alpha\beta$, in order to obtain a value for $\tau = \alpha\beta$. A fit of one of the inverted and normalized averaged voltage traces is given in Fig. 3a.

1. Berger, L. Emission of spin waves by a magnetic multilayer traversed by a current. *Phys. Rev. B* **54**, 9353 (1996).
2. Slonczewski, J. C. Current-driven excitation of magnetic multilayers. *J. Magn. Magn. Mater.* **159**, L1 (1996).
3. Grollier, J. *et al.* Switching a spin valve back and forth by current-induced domain wall motion. *Appl. Phys. Lett.* **83**, 509 (2003).
4. Kläui, M. *et al.* Domain wall motion induced by spin polarized currents in ferromagnetic ring structures. *Appl. Phys. Lett.* **83**, 105 (2003).
5. Grollier, J. *et al.* Magnetic domain wall motion by spin transfer. *C. R. Physique* **12**, 309 (2011).
6. Malinowski, G., Boulle, O. & Kläui, M. Current-induced domain wall motion in nanoscale ferromagnetic elements. *J. Phys. D: Appl. Phys.* **44**, 384005 (2011).
7. Parkin, S. S. P., Hayashi, M. & Thomas, L. Magnetic domain-wall racetrack memory. *Science* **320**, 190 (2008).
8. Hayashi, M., Thomas, L., Moriya, R., Rettner, C. & Parkin, S. S. P. Current-controlled magnetic domain-wall nanowire shift register. *Science* **320**, 209 (2008).
9. Kim, K. J. *et al.* Electric control of multiple domain walls in Pt/Co/Pt nanotracks with perpendicular magnetic anisotropy. *Appl. Phys. Express* **3**, 083001 (2010).
10. Zhao, W., Ravelosona, D., Klein, J. O. & Chappert, C. Domain wall shift register-based reconfigurable logic. *IEEE Trans. Mag.* **47**, 2966 (2011).
11. Franken, J. H., Swagten, H. J. M. & Koopmans, B. Shift registers based on magnetic domain wall ratchets with perpendicular anisotropy. *Nat. Nanotechnol.* **7**, 499 (2012).
12. Fukami, S., Suzuki, T., Ohshima, N., Nagahara, K. & Ishiwata, N. Intrinsic threshold current density of domain wall motion in nanostrips with perpendicular magnetic anisotropy for use in low-write-current MRAMs. **44**, 2539 (2008).
13. Fukami, S. *et al.* Low-current perpendicular domain wall motion cell for scalable high-speed mram. In *VLSI Technology, 2009 Symposium on*, 230–231 (2009).
14. Fukami, S. *et al.* Current-induced domain wall motion in perpendicularly magnetized CoFeB nanowire. *Appl. Phys. Lett.* **98**, 082504 (2011).
15. Wang, X., Chen, Y., Xi, H., Li, H. & Dimitrov, D. Spintronic memristor through spin-torque-induced magnetization motion. *IEEE Elec. Dev. Lett.* **30**, 294 (2009).
16. Chanthbouala, A. *et al.* Vertical-current-induced domain-wall motion in MgO-based magnetic tunnel junctions with low current densities. *Nat. Phys.* **7**, 626 (2011).
17. Münchenberger, J., Reiss, G. & Thomas, A. A memristor based on current-induced domain-wall motion in a nanostructured giant magnetoresistance device. *J. Appl. Phys.* **111**, 07D303 (2012).
18. Zhang, S. & Li, Z. Roles of nonequilibrium conduction electrons on the magnetization dynamics of ferromagnets. *Phys. Rev. Lett.* **93**, 127204 (2004).
19. Thiaville, A., Nakatani, Y., Miltat, J. & Suzuki, Y. Micromagnetic understanding of current-driven domain wall motion in patterned nanowires. *Europhys. Lett.* **69**, 990 (2005).
20. Gilmore, K., Garate, I., MacDonald, A. H. & Stiles, M. D. First-principles calculation of the nonadiabatic spin transfer torque in Ni and Fe. *Phys. Rev. B* **84**, 224412 (2011).
21. Petitjean, C., Luc, D. & Waintal, X. Unified drift-diffusion theory for transverse spin currents in spin valves, domain walls and other textured magnets. *Phys. Rev. Lett.* **109**, 117204 (2012).
22. Heyne, L. *et al.* Direct determination of large spin-torque nonadiabaticity in vortex core dynamics. *Phys. Rev. Lett.* **105**, 187203 (2010).
23. Hayashi, M. *et al.* Current driven domain wall velocities exceeding the spin angular momentum transfer rate in permalloy nanowires. *Phys. Rev. Lett.* **98**, 037204 (2007).
24. Meier, G. *et al.* Direct imaging of stochastic domain-wall motion driven by nanosecond current pulses. *Phys. Rev. Lett.* **98**, 187202 (2007).
25. Miron, I. M. *et al.* Current-driven spin torque induced by the rashba effect in a ferromagnetic metal layer. *Nature Materials* **9**, 230 (2010).
26. Miron, I. M. *et al.* Fast current-induced domain-wall motion controlled by the rashba effect. *Nature Mater.* **10**, 419 (2011).
27. Emori, S., Bono, D. C. & Beach, G. S. D. Interfacial current-induced torques in Pt/Co/GdOx. *Appl. Phys. Lett.* **101**, 042405 (2012).
28. Thiaville, A., Rohart, S., Jué, E., Cros, V. & Fert, A. Dynamics of dzyaloshinskii domain walls in ultrathin magnetic films. *Europhys. Lett.* **100**, 57002 (2012).

29. Khvalkovskiy, A. *et al.* High domain wall velocities due to spin currents perpendicular to the plane. *Phys. Rev. Lett.* **102**, 067206 (2009).
30. Rebei, A. & Mryasov, O. Dynamics of a trapped domain wall in a spin-valve nanostructure with current perpendicular to the plane. *Phys. Rev. B* **74**, 014412 (2006).
31. Martínez-Boubeta, C. Effect of the bias current on the magnetic field switching in micrometer AlO*x*-based tunnel junctions. *J. Appl. Phys* **102**, 043905 (2007).
32. Cucchiara, J. *et al.* Telegraph noise due to domain wall motion driven by spin current in perpendicular magnetized nanopillars. *Appl. Phys. Lett.* **94**, 102503 (2009).
33. Bernstein, D. P. *et al.* Nonuniform switching of the perpendicular magnetization in a spin-torque-driven magnetic nanopillar. *Phys. Rev. B* **83**, 180410 (2011).
34. Boone, C. T. *et al.* Rapid domain wall motion in permalloy nanowires excited by a spin-polarized current applied perpendicular to the nanowire. *Phys. Rev. Lett.* **104**, 097203 (2010).
35. Herranz, D. *et al.* Low frequency noise due to magnetic inhomogeneities in submicron Fe-CoB/MgO/FeCoB magnetic tunnel junctions. *Appl. Phys. Lett.* **99**, 062511 (2011).
36. Yuasa, S., Nagahama, T., Fukushima, A., Suzuki, Y. & Ando, K. Giant room-temperature magnetoresistance in single-crystal Fe/MgO/Fe magnetic tunnel junctions. *Nature Mater.* **3**, 868 (2004).
37. Parkin, S. S. P. *et al.* Giant tunnelling magnetoresistance at room temperature with MgO (100) tunnel barriers. *Nat. Mater.* **3**, 862 (2004).
38. Kondou, K., Ohshima, N., Kasai, S., Nakatani, Y. & Ono, T. Single shot detection of the magnetic domain wall motion by using tunnel magnetoresistance effect. *Appl. Phys. Express* **1**, 061302 (2008).
39. Cui, Y.-T. *et al.* Single-shot time-domain studies of spin-torque-driven switching in magnetic tunnel junctions. *Phys. Rev. Lett.* **104**, 097201 (2010).
40. Nakatani, Y., Thiaville, A. & Miltat, J. Head-to-head domain walls in soft nano-strips: a refined phase diagram. *J. Magn. Magn. Mater.* **290**, 750 (2005).
41. Burrowes, C. *et al.* Non-adiabatic spin-torques in narrow magnetic domain walls. *Nat. Phys.* **6**, 17 (2010).
42. Bedau, D. *et al.* Spin-transfer pulse switching: From the dynamic to the thermally activated regime. *Appl. Phys. Lett.* **97**, 262502 (2010).
43. Hogg, R. V. *Introduction to Mathematical Statistics* (Pearson Education, Inc., 2005).
44. Devolder, T. *et al.* Single-shot time-resolved measurements of nanosecond-scale spin-transfer induced switching: Stochastic versus deterministic aspects. *Phys. Rev. Lett.* **100**, 057206 (2008).
45. Kim, J.-V. & Burrowes, C. Influence of magnetic viscosity on domain wall dynamics under spin-polarized currents. *Phys. Rev. B* **80**, 214424 (2009).
46. Hayashi, M. *et al.* Influence of current on field-driven domain wall motion in permalloy nanowires from time resolved measurements of anisotropic magnetoresistance. *Physical Review Letters* **96**, 197207 (2006).
47. Yuasa, S. & Djayaprawira, D. D. Giant tunnel magnetoresistance in magnetic tunnel junctions with a crystalline MgO(111) barrier. *J. Phys. D: Appl. Phys.* **40**, R337–R354 (2007).

Acknowledgements

The authors acknowledge financial support from the European Research Council (Starting Independent Researcher Grant No. ERC 2010 Stg 259068) and the French ANR grant ESPERADO 11-BS10-008.

Author contributions

J.G., P.J.M. and V.C. conceived the experiments; P.J.M., J.S. and A.C. carried out the measurements and analyzed the data with the help of J.G. and V.C.; R.M. and A.C. performed the micromagnetic simulations with help from J.G. and K.A.Z.; K.N., Y.N., H.M. and K.T. prepared the magnetic films; A.F., K.Y. and H.K. fabricated the devices; P.J.M., A.C. and J.G. wrote the paper with discussions and comments from V.C., A.A., S.Y. and A.F.

Additional information

Supplementary information accompanies this paper at http://www.nature.com/scientificreports

Competing financial interests: The authors declare no competing financial interests.

License: This work is licensed under a Creative Commons Attribution-NonCommercial-NoDerivs 3.0 Unported License. To view a copy of this license, visit http://creativecommons.org/licenses/by-nc-nd/3.0/

How to cite this article: Metaxas, P.J. *et al.* High domain wall velocities via spin transfer torque using vertical current injection. *Sci. Rep.* **3**, 1829; DOI:10.1038/srep01829 (2013).